MCB
Journals.ASM.org

A Role for SMN Exon 7 Splicing in the Selective Vulnerability of Motor Neurons in Spinal Muscular Atrophy

Matteo Ruggiu,[a,b] Vicki L. McGovern,[c] Francesco Lotti,[a,b] Luciano Saieva,[a,b] Darrick K. Li,[a,b] Shingo Kariya,[a,b,d] Umrao R. Monani,[a,b,d] Arthur H. M. Burghes,[c] and Livio Pellizzoni[a,b]

Department of Pathology and Cell Biology, Columbia University, New York, New York, USA[a]; Center for Motor Neuron Biology and Disease, Columbia University, New York, New York, USA[b]; Department of Molecular and Cellular Biochemistry, The Ohio State University, Columbus, Ohio, USA[c]; and Department of Neurology, Columbia University, New York, New York, USA[d]

Spinal muscular atrophy (SMA) is an inherited motor neuron disease caused by homozygous loss of the *Survival Motor Neuron 1* (*SMN1*) gene. In the absence of *SMN1*, inefficient inclusion of exon 7 in transcripts from the nearly identical *SMN2* gene results in ubiquitous SMN decrease but selective motor neuron degeneration. Here we investigated whether cell type-specific differences in the efficiency of exon 7 splicing contribute to the vulnerability of SMA motor neurons. We show that normal motor neurons express markedly lower levels of full-length SMN mRNA from *SMN2* than do other cells in the spinal cord. This is due to inefficient exon 7 splicing that is intrinsic to motor neurons under normal conditions. We also find that SMN depletion in mammalian cells decreases exon 7 inclusion through a negative feedback loop affecting the splicing of its own mRNA. This mechanism is active *in vivo* and further decreases the efficiency of exon 7 inclusion specifically in motor neurons of severe-SMA mice. Consistent with expression of lower levels of full-length SMN, we find that SMN-dependent downstream molecular defects are exacerbated in SMA motor neurons. These findings suggest a mechanism to explain the selective vulnerability of motor neurons to loss of *SMN1*.

Spinal muscular atrophy (SMA) is an autosomal recessive disorder characterized by degeneration of motor neurons (MNs) in the spinal cord and by skeletal muscle atrophy (8, 38, 44). SMA is the most common genetic cause of infant mortality and is classified into three types based on the age of onset and clinical severity (50, 56). Regardless of disease severity, all SMA patients have homozygous deletions or mutations in the *Survival Motor Neuron 1* (*SMN1*) gene—the SMA-determining gene—and retain at least one copy of the nearly identical *SMN2* gene (33). While the *SMN1* gene produces full-length transcripts, the *SMN2* gene mainly produces an alternatively spliced mRNA lacking exon 7 (SMNΔ7). Since the SMNΔ7 protein is unstable and rapidly degraded (32, 36), the low levels of full-length functional SMN produced by the *SMN2* gene cannot compensate for the loss of *SMN1*, resulting in SMA. Thus, SMA is caused by decreased expression of SMN protein, and correspondingly, disease severity correlates well with the degree of SMN reduction in SMA patients (19, 34). Importantly, the *SMN2* gene copy number varies in the human population and acts as the principal disease modifier in SMA because the presence of more *SMN2* copies generally coincides with a milder clinical outcome (41). Studies of human SMA patients and animal models of disease indicate that low SMN levels from *SMN2* are sufficient for normal function of most cells but not motor neurons (8, 44). However, the reason for the selective vulnerability of motor neurons to SMN deficiency is unknown.

Since the efficiency of exon 7 splicing determines the amount of functional SMN produced by *SMN2*, the mechanisms underlying the alternative splicing of exon 7 in *SMN1* and *SMN2* mRNAs have been subject to extensive studies. This is for two main reasons: the critical relevance of exon 7 splicing in SMA etiology and its role as a potential target of therapeutic intervention through splicing correction. To date, an array of *cis*-acting elements and *trans*-acting factors has been implicated in the regulation of SMN exon 7 splicing (5, 51, 58). Most importantly, a single nucleotide difference between *SMN1* and *SMN2*—a C-to-T transition at position +6 of exon 7—has been found to be largely responsible for the differential inclusion of exon 7 in SMN transcripts (37, 45). Whereas the C in *SMN1* exon 7 is thought to form an exonic splicing enhancer (ESE) element that is bound by ASF/SF2 to promote exon inclusion (12, 13), the T at the same position in *SMN2* exon 7 not only disrupts the ESE motif but also creates an exonic splicing silencer (ESS) that is bound by hnRNP A1 and Sam68, causing enhanced exon skipping (30, 51). Recent studies identified sequence variants of *SMN2* that increase exon 7 inclusion and are associated with reduced disease severity in patients (6, 55, 60), further underscoring the importance of exon 7 splicing in SMA pathology.

The critical role of RNA splicing in SMA etiology is not limited to the regulation of exon 7 inclusion but also involves the function of the SMN protein. SMN and at least eight additional proteins termed Gemin2 to Gemin8 and Unrip form a large multiprotein complex known as the SMN complex (2, 10, 11, 16, 17, 25, 35, 53). The only molecularly defined cellular function of the SMN complex is in the biogenesis of small nuclear ribonucleoproteins (snRNPs) (3, 40, 47, 52), which are the essential components of pre-mRNA splicing machinery. Spliceosomal snRNPs of the Sm class are comprised of one snRNA molecule (U1, U2, U4, U5, U11, U12, and U4atac) and seven common Sm proteins, as well as

Received 5 August 2011 **Returned for modification** 7 September 2011
Accepted 19 October 2011
Published ahead of print 28 October 2011
Address correspondence to Livio Pellizzoni, lp2284@columbia.edu.
Supplemental material for this article may be found at http://mcb.asm.org/.

doi:10.1128/MCB.06077-11

auxiliary factors specific to each snRNA (61). The activity of the SMN complex is required for the assembly of the heptameric core of Sm proteins on snRNAs that occurs in the cytoplasm (14, 21, 43, 54). Our previous studies in mouse models of SMA have demonstrated a direct correlation between disease severity and the degree of snRNP assembly defects caused by SMN deficiency in the spinal cord (22). Impairment of this essential, SMN-dependent pathway decreases snRNP levels in tissues of severe-SMA mice (22, 64). Importantly, restoration of normal snRNP levels coincides with phenotypic correction in animal models of SMA (62, 63). Thus, increasing evidence links SMN-dependent disruption of snRNP biogenesis to SMA pathology (15, 52). However, the identity of SMN target mRNAs whose defective splicing may contribute to motor neuron dysfunction in SMA remains elusive.

To date, therefore, a dual connection between RNA splicing and SMA etiology has emerged. On one hand, the decrease in SMN protein levels that causes SMA in the absence of *SMN1* is due to inefficient splicing of exon 7 in transcripts from *SMN2*. On the other hand, the function of SMN in the assembly of snRNPs is essential for RNA splicing and impaired in SMA. In this work, we have tested the hypothesis that cell type-specific differences in the efficiency of exon 7 splicing may contribute to the selective vulnerability of motor neurons in SMA. We show that normal motor neurons express markedly lower levels of full-length SMN mRNA from the *SMN2* gene than other cell types in the spinal cord and that this is due to particularly inefficient exon 7 inclusion. We also highlight a negative feedback loop whereby SMN-dependent changes in the snRNP abundance decrease exon 7 splicing in mammalian cells, consistent with the conclusions of a recent study (29). Importantly, analysis of severe-SMA mice revealed that this feedback mechanism is active *in vivo* in motor neurons but not in other spinal cord cells. Consistent with a greater reduction in SMN levels upon loss of *SMN1*, we provide evidence that downstream molecular defects linked to SMN deficiency are strongly and specifically exacerbated in SMA motor neurons. Our findings identify *SMN2* exon 7 inclusion as an SMN-dependent splicing event that is relevant to SMA pathology. They also uncover a plausible mechanism to explain the selective vulnerability of motor neurons in SMA that is based on cell type-specific differences in the efficiency of exon 7 inclusion and their reduced ability to produce functional SMN protein from the *SMN2* gene compared to other spinal cells.

MATERIALS AND METHODS

Tissue culture and DNA transfection. NIH 3T3 cells were grown in Dulbecco modified Eagle medium (DMEM) with high glucose (Gibco) containing 10% fetal bovine serum (HyClone), 2 mM glutamine (Gibco), and 0.1 mg/ml gentamicin (Gibco). RNA interference (RNAi) was induced where needed by addition to the growth medium of doxycycline (Dox; Fisher) at a final concentration of 100 ng/ml, and cells were collected after 5 days. For transient-transfection experiments, 4×10^5 cells were transfected with 4 μg of either *SMN1* or *SMN2* splicing reporter constructs (30) using PolyFect transfection reagent (Qiagen) according to the manufacturer's instructions. Following incubation for 12 h at 37°C, the growth medium was changed and cells were incubated for an additional 24 h at 37°C prior to collection.

NIH 3T3 cell lines. The NIH 3T3 cell lines used in this study were generated through lentiviral transduction followed by antibiotic selection and cloning by limiting dilution. With the exception of commercially available pLenti6/TR (Invitrogen)—which constitutively expresses the tetracycline-dependent repressor (TR) protein under the control of the cytomegalovirus (CMV) promoter—all other lentiviral constructs were generated by standard cloning techniques using pRRLSIN.cPPT.PGK-GFP.WPRE as a backbone (Addgene plasmid 12252). Viral stocks pseudotyped with the vesicular stomatitis G protein (VSV-G) were prepared by transient cotransfection of 293T cells using the ViraPower lentiviral packaging mix (Invitrogen) according to the manufacturer's instructions. NIH 3T3-Smn_{RNAi} cells were generated by serial transduction of wild-type NIH 3T3 cells with pLenti6/TR and a lentiviral construct expressing a short hairpin RNA (shRNA) targeting mouse Smn mRNA (5′-GAAGA AUGCCACAACUCCC-3′) under the control of a tetracycline-regulated H1 promoter. NIH 3T3-SMN/Smn_{RNAi} cells were generated by transduction of NIH 3T3-Smn_{RNAi} cells with a lentiviral construct constitutively expressing epitope-tagged human SMN (Flag and Strep fused in tandem at the amino terminus) under the control of the phosphoglycerate kinase (PGK) promoter. NIH 3T3-SmB_{RNAi} cells were generated by serial transduction of wild-type NIH 3T3 cells with pLenti6/TR and a lentiviral construct expressing an shRNA targeting mouse SmB mRNA (5′-GCAAGA TGCTGCAGCACAT-3′) under the control of a tetracycline-regulated H1 promoter.

Mouse breeding and tissue collection. FVB.Cg-Tg(*SMN2*)89Ahmb Smn1tm1Msd/J (JAX stock no. 005024) mice were interbred to obtain severe-SMA ($Smn^{-/-}$; $SMN2^{+/+}$) mice (46). FVB.Cg-Tg(*SMN2**delta7)4299Ahmb Tg(*SMN2*)89Ahmb Smn1tm1Msd/J (JAX stock no. 005025) mice were interbred to obtain Δ7 SMA ($Smn^{-/-}$; $SMN2^{+/+}$; $SMN\Delta7^{+/+}$) mice (32). Δ7 SMA mice specifically expressing green fluorescent protein (GFP) in motor neurons were generated by crossing FVB.Cg-Tg(*SMN2**delta7)4299Ahmb Tg(*SMN2*)89Ahmb Smn1tm1Msd/J (JAX stock no. 005025) mice to B6.Cg-Tg(Hlxb9-GFP)1Tmj/J (JAX stock no. 005029) mice. The resulting carrier mice ($Smn^{+/-}$; $SMN2^{+/+}$; $SMN\Delta7^{+/+}$; HB9:$GFP^{+/-}$) were interbred for more than 10 generations to obtain Δ7 SMA ($Smn^{-/-}$; $SMN2^{+/+}$; $SMN\Delta7^{+/+}$; HB9:$GFP^{+/-}$) mice. The phenotype of these mice was no different from that of line 005025. All experiments were conducted in accordance with the protocols described in the National Institutes of Health *Guide for the Care and Use of Animals* and were approved by the Institutional Laboratory Animal Care and Use Committee of Ohio State University and Columbia University. Spinal cord tissue from control and SMA mice was rapidly dissected and immediately frozen in liquid nitrogen. A tail biopsy specimen was also taken from each mouse and used for genotyping as previously described (22). All tissue samples were stored at −80°C until use.

Immunohistochemistry. Immunohistochemistry experiments were carried out using normal ($Smn^{+/+}$; $SMN2^{+/+}$; $SMN\Delta7^{+/+}$) and Δ7 SMA ($Smn^{-/-}$; $SMN2^{+/+}$; $SMN\Delta7^{+/+}$) mice at postnatal day 10. Mice sacrificed by CO_2 gas inhalation were transcardially perfused first with phosphate-buffered saline (PBS) and then with 4% paraformaldehyde (PFA)-0.1 M phosphate buffer (PB). Spinal cords were dissected, post-fixed for 2 h in 4% PFA-0.1 M PB, cryoprotected for 3 days in 30% sucrose, and then embedded in Tissue-Tek O.C.T. compound (Sakura Finetechnical, Tokyo, Japan). T10 transverse sections (20 μm) of the spinal cord cut on a cryostat were blocked for 30 min in a solution containing 3% bovine serum albumin (BSA), 5% donkey serum, and 1% Triton X-100 and then incubated for 2 days with a mouse monoclonal anti-SmB antibody (18F6; 1:200) and a rabbit polyclonal anti-Hb9 antibody (Abcam; 1:16,000). After several washes, the sections were incubated for 3 h with an Alexa Fluor 488-conjugated donkey anti-mouse IgG and an Alexa Fluor 594-conjugated donkey anti-rabbit IgG (Invitrogen; 1:500) before being mounted in Vectashield (Vector Laboratories, Burlingame, CA). Images were acquired on a laser scanning confocal microscope (Bio-Rad 1024; Bio-Rad, Hercules, CA) under identical exposure and gain settings. Hb9 and SmB levels in the nucleus of motor neurons were quantified from Z-stack confocal images by measuring mean fluorescence intensity per area using ImageJ 1.37v software.

LCM. Spinal cord sections (L1 to L5) were harvested from control ($Smn^{+/-}$; $SMN2^{+/+}$; $SMN\Delta7^{+/+}$; HB9:$GFP^{+/-}$) and Δ7 SMA ($Smn^{-/-}$;

SMN2$^{+/+}$; SMNΔ7$^{+/+}$; HB9:GFP$^{+/-}$) mice at postnatal day 6, mounted, and flash frozen in liquid nitrogen-cooled isopentane. Spinal cords were cryosectioned (14 μm) and made to adhere to UV-treated PEN membrane slides (Zeiss). Tissue sections were immediately fixed in methanol for 30 s, Nissl stained in 1% cresyl violate acetate for 1 min, and immediately stored at −80°C. Laser capture microdissection (LCM) was performed with the Palm Microbeam (Carl Zeiss MicroImaging) under 10× magnification. Motor neurons were identified by size and position in the ventral horn of the spinal cord. Approximately 500,000 μm^2 of motor neuron tissue was collected per sample. For each sample, an additional 500,000 μm^2 of non-motor neuron tissue was collected from the dorsal horn of the same spinal cord sections.

RNA purification and RT-PCR analysis. RNA from NIH 3T3 cells and whole spinal cord tissue was extracted with TRIzol reagent (Invitrogen) and digested with DNase I (Ambion). RNA was reverse transcribed using the RevertAid first-strand cDNA kit (Fermentas). RNA from LCM samples was purified using the RNAqueous-Micro kit (Ambion; AM1931). One round of linear amplification was performed with the MessageAmp II aRNA amplification kit (Ambion; AM1751) according to the manufacturer's instructions. For analysis of exon 7 splicing by semiquantitative radioactive reverse transcription-PCR (RT-PCR), the forward primer was end labeled using T4 polynucleotide kinase (New England BioLabs) and [γ-^{32}P]ATP (Amersham). PCR products were amplified using AmpliTaq Gold DNA polymerase (Roche), resolved on a 6% polyacrylamide-8 M urea gel, and subjected to autoradiography. Quantification of radiolabeled PCR products was carried out using a Typhoon PhosphorImager (Molecular Dynamics). The linear range of amplification was determined by independent PCRs for each experiment. Primers used for radioactive RT-PCR analysis are listed in Table S1 in the supplemental material. For real-time RT-quantitative PCR (RT-qPCR) analysis, qPCRs were carried out using Power SYBR green PCR master mix (Applied Biosystems) in a Realplex^4 Mastercycler (Eppendorf). The qPCR primers used in this study are listed in Table S1 in the supplemental material.

Antibodies. The antibodies used in this study were as follows: anti-SMN clone 8 (BD Transduction Laboratories), anti-glyceraldehyde-3-phosphate dehydrogenase (anti-GAPDH) (Chemicon), anti-Gemin8 1F8 (11), anti-hnRNPR/Q 18E4 (Sigma), anti-hnRNPA1 4B10 (Sigma), anti-Sam68 (Santa Cruz), anti-ASF/SF2 (Santa Cruz), anti-Tra2-β1 (26), anti-SRp20 (Santa Cruz), anti-TDP43 (Proteintech Group), anti-SR proteins (Zymed), anti-SmB 18F6 (11), anti-Sm Y12 (Lab Vision), anti-Hb9 (Abcam), antitubulin DM 1A (Sigma), and anti-Flag M2 (Sigma).

Western blotting. Cells were lysed in SDS sample buffer (2% SDS, 10% glycerol, 5% β-mercaptoethanol, 60 mM Tris-HCl, pH 6.8, bromophenol blue), passed through a 27-gauge needle five times, and sonicated. Protein extracts were quantified using the RC DC protein assay (Bio-Rad). Samples were run on a 12% SDS-PAGE gel and transferred onto a Trans-Blot transfer medium nitrocellulose membrane (Bio-Rad) using a TE77x semidry transfer unit (Hoefer) using 1× Tris-glycine buffer (Bio-Rad) containing 20% methanol. Membranes were stained with 0.1% (wt/vol) Ponceau S and 5% acetic acid, destained in distilled H_2O, and blocked for 1 h at room temperature with 5% nonfat dry milk (LabScientific) in PBS containing 0.1% Tween 20 (Acros). Incubation with primary antibody was performed in PBS containing 0.1% Tween 20 for 1 h at room temperature. Membranes were washed 3 times for 10 min with PBS containing 0.1% Tween 20 at room temperature. Incubation with secondary antibodies conjugated to horseradish peroxidase was performed in PBS containing 0.1% Tween 20 for 1 h at room temperature. Membranes were washed 3 times for 10 min with PBS containing 0.1% Tween 20 at room temperature. Chemiluminescence was carried out using a SuperSignal West Pico chemiluminescent substrate (Thermo Scientific) according to the manufacturer's instructions. Signal was detected by autoradiography using Full Speed Blue sensitive medical X-ray film (Ewen Parker X-Ray Corporation).

RNA pulldown. The *SMN1* and *SMN2* RNA probes used in this study have been described elsewhere (39). Biotinylated *SMN1* and *SMN2* RNA probes were transcribed from DNA templates using the MEGAshortscript T7 transcription kit (Ambion) in the presence of 5 mM ATP/CTP/GTP, 3.75 mM UTP, 1.25 mM biotin-UTP, and [α-^{32}P]UTP (3,000 Ci/mmol). After digestion with Turbo DNase I (Ambion), biotinylated RNAs were separated on an 8% polyacrylamide-8 M urea gel and purified from the gel using RNA elution buffer (300 mM sodium acetate, 0.1% SDS, 1 mM EDTA) in the presence of 10% phenol (phenol-chloroform-isoamyl alcohol, 25:24:1) overnight at room temperature. Whole-cell extracts from NIH 3T3 cells were prepared in buffer E (20 mM HEPES-KOH, pH 7.9, 100 mM KCl, 0.2 mM EDTA, 10% glycerol) containing 1 mM dithiothreitol (DTT), complete EDTA-free protease inhibitors (Roche), and PhosStop phosphatase inhibitors (Roche) as previously described (31). Protein concentration was measured using the Bradford assay (Bio-Rad). For each pulldown, 100 μg of whole-cell extract was incubated with 500 ng of biotinylated RNA in buffer E containing 0.5 mM ATP, 20 mM creatine phosphate, 1.6 mM $MgCl_2$, and 1 μl of RNasin Plus RNase inhibitor (Promega) for 30 min at 30°C. After incubation, RNA-protein complexes were isolated with protein G streptavidin Sepharose High Performance beads (GE Healthcare) in a final volume of 1 ml of RSB-100 (10 mM Tris-HCl, pH 7.4, 2.5 mM $MgCl_2$, 100 mM NaCl) containing 0.1% Nonidet P-40 (NP-40; Accurate Chemical and Scientific Corp.) for 2 h at 4°C while rotating. Beads were washed 5 times with 1 ml of RSB-100 containing 0.1% NP-40, and bound proteins were eluted by boiling in SDS-PAGE buffer prior to Western blot analysis.

snRNP analysis. For *in vitro* snRNP assembly experiments, cell extracts from NIH 3T3 cells were prepared in ice-cold reconstitution buffer (20 mM HEPES-KOH, pH 7.9, 50 mM KCl, 5 mM $MgCl_2$, 0.2 mM EDTA, 5% glycerol) containing 0.01% NP-40 as previously described (22). Radioactive U1 snRNA was prepared by transcription from a linearized template DNA in the presence of [α-^{32}P]UTP (3,000 Ci/mmol) and m7G cap analogue (New England BioLabs) and then purified from denaturing polyacrylamide gels according to standard procedures. *In vitro* snRNP assembly assays with freshly prepared NIH 3T3 cell extracts (10 μg, 20 μg, or 40 μg) were carried out in a volume of 20 μl of reconstitution buffer containing 0.01% NP-40, 10,000 cpm of radioactive U1 snRNA, 2.5 mM ATP, and 10 μM *Escherichia coli* tRNA for 1 h at 30°C. Following addition of heparin and urea to final concentrations of 5 mg/ml and 2 M, respectively, reaction mixtures were analyzed by electrophoresis on 6% polyacrylamide native gels at 4°C and autoradiography (54).

Analysis of steady-state levels of endogenous snRNPs was carried out as previously described (22). Briefly, NIH 3T3 cell extracts (200 μg) were immunoprecipitated with anti-Sm (Y12) antibodies in RSB-500 buffer (500 mM NaCl, 10 mM Tris-HCl, pH 7.4, 2.5 mM $MgCl_2$) containing 0.1% NP-40, EDTA-free protease inhibitor cocktail (Roche), and phosphatase inhibitors (50 mM NaF, 0.2 mM Na_3VO_4) for 2 h at 4°C. After extensive washing, snRNAs were 3′ end labeled in the presence of [^{32}P]pCp (3,000 Ci/mmol) and T4 RNA ligase (Roche), followed by electrophoresis on 6% polyacrylamide-8 M urea gels and autoradiography. Quantification was carried out using a Typhoon PhosphorImager (Molecular Dynamics).

Immunofluorescence analysis. NIH 3T3-Smn$_{RNAi}$ cells cultured on glass coverslips in 24-well plates either in the presence or in the absence of doxycycline were washed briefly with PBS, fixed with 4% PFA-PBS for 30 min at room temperature, and permeabilized with 0.5% Triton X-100–PBS for 5 min on ice. Blocking and incubation with both primary and secondary antibodies were performed using 3% BSA-PBS for 1 h at room temperature. Images were collected with a Leica SP5 confocal microscope.

Statistical analysis. Statistical analysis was carried out using the unpaired Student *t* test and the Prism 5 (GraphPad) software. *P* values are indicated as follows: *, $P < 0.05$; **, $P < 0.01$; ***, $P < 0.001$. Unless otherwise stated, all quantification data are plotted as means and standard errors of the means (SEM) from independent experiments.

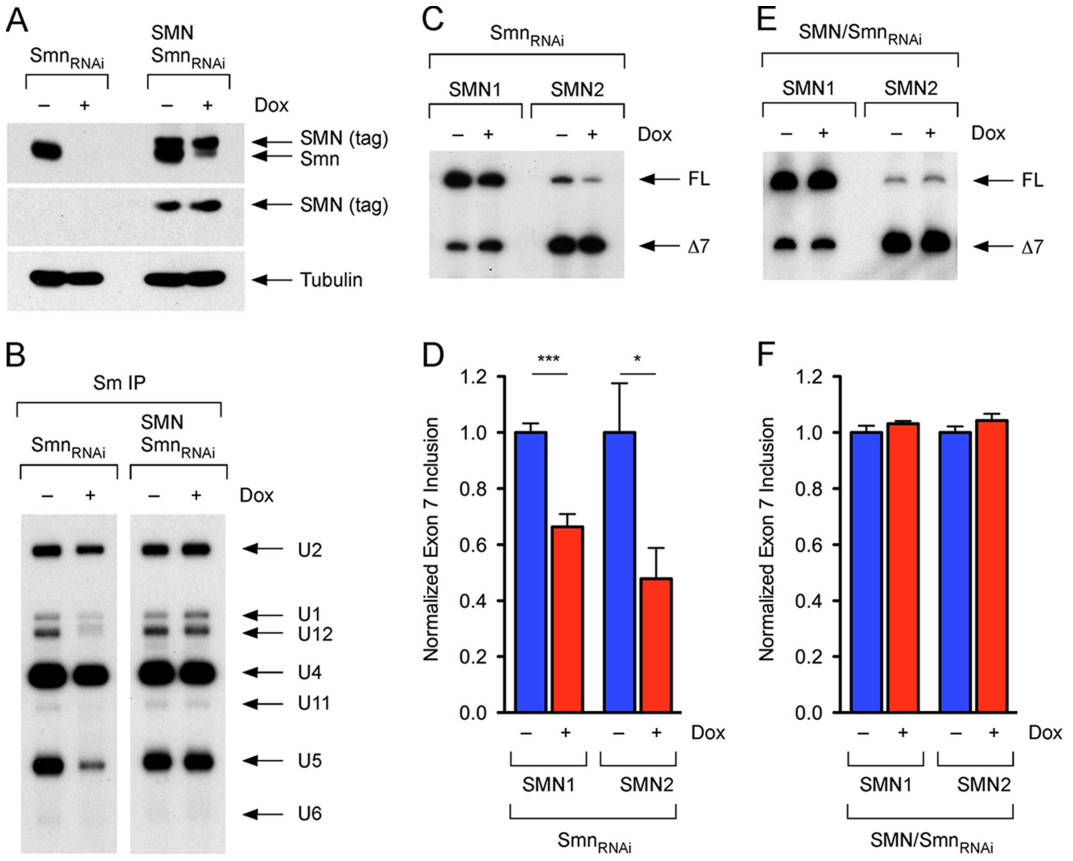

FIG 1 SMN deficiency impairs exon 7 splicing. (A) NIH 3T3 cell lines with regulated knockdown of mouse Smn. Western blot analysis of NIH 3T3-Smn$_{RNAi}$ and NIH 3T3-SMN/Smn$_{RNAi}$ cells cultured for 5 days without (−) or with (+) doxycycline (Dox). Blots were probed with an antibody that recognizes both mouse and human SMN proteins to monitor knockdown efficiency, with an anti-Flag antibody to detect epitope-tagged human SMN, and with an antibody against tubulin as a loading control. Addition of Dox to the growth medium specifically induces shRNA expression and consequently RNAi-mediated knockdown of endogenous mouse Smn protein. The slower migration of RNAi-resistant human SMN is due to the presence of an epitope tag at the amino terminus as indicated by its detection with anti-Flag antibodies. (B) Smn deficiency decreases the levels of spliceosomal snRNPs in NIH 3T3 cells. Extracts from NIH 3T3-Smn$_{RNAi}$ and NIH 3T3-SMN/Smn$_{RNAi}$ cells cultured for 5 days either without (−) or with (+) Dox were immunoprecipitated with an anti-Sm antibody followed by 3′ end labeling of RNA, denaturing gel electrophoresis, and autoradiography. Known snRNA species are indicated on the right. Note that most U6 snRNAs harbor a 2′,3′-cyclic phosphate end that is not labeled using this assay. Quantification of snRNP levels from independent experiments is shown in Fig. S2 in the supplemental material. (C) SMN deficiency decreases the efficiency of exon 7 inclusion in NIH 3T3 cells. Radioactive RT-PCR analysis of exon 7 splicing following transfection of *SMN1* or *SMN2* minigene reporters into NIH 3T3-Smn$_{RNAi}$ cells cultured without (−) or with (+) Dox. Arrows point to exon 7-included (FL) and exon 7-skipped (Δ7) SMN mRNAs. (D) Quantification of the efficiency of exon 7 inclusion in NIH 3T3-Smn$_{RNAi}$. Blue and red bars correspond to results from NIH 3T3 cells cultured without (−) or with (+) Dox, respectively. Values represent means and SEM from independent experiments ($n = 4$; *, $P < 0.05$; ***, $P < 0.001$) as in panel C. Data were normalized relative to −Dox set as 1. (E) Expression of human SMN corrects exon 7 splicing defects caused by depletion of endogenous mouse Smn in NIH 3T3 cells. Radioactive RT-PCR analysis of SMN exon 7 splicing following transfection with either *SMN1* or *SMN2* minigene reporters into NIH 3T3-SMN/Smn$_{RNAi}$ cells cultured without (−) or with (+) Dox. (F) Quantification of the efficiency of exon 7 inclusion in NIH 3T3-SMN/Smn$_{RNAi}$ cells. Blue and red bars correspond to results from NIH 3T3 cells cultured without (−) or with (+) Dox, respectively. Values represent means and SEM from independent experiments ($n = 3$) as in panel E. Data were normalized relative to −Dox set as 1.

RESULTS

SMN deficiency impairs exon 7 inclusion in SMN mRNAs. We sought to investigate the effects of SMN deficiency on splicing of exon 7 using a stable NIH 3T3 cell line (NIH 3T3-Smn$_{RNAi}$) in which expression of an shRNA against endogenous mouse Smn mRNA is triggered by addition of doxycycline to the culture medium. Western blot analysis showed that treatment of NIH 3T3-Smn$_{RNAi}$ cells with doxycycline for 5 days strongly reduces the levels of the Smn protein (Fig. 1A). To control for nonspecific, off-target effects of shRNA expression, NIH 3T3-Smn$_{RNAi}$ cells were further engineered to constitutively express an epitope-tagged isoform of human SMN that is resistant to RNAi (NIH 3T3-SMN/Smn$_{RNAi}$). Figure 1A shows that human SMN is expressed at levels comparable to those of endogenous Smn and is not affected by doxycycline-dependent RNAi induction in NIH 3T3-SMN/Smn$_{RNAi}$ cells. Consistent with previous studies (22, 64), immunoprecipitation experiments with anti-Sm antibodies revealed that Smn depletion in NIH 3T3 cells causes a profound alteration in the levels of spliceosomal snRNPs and that this defect is corrected by ectopic expression of human SMN (Fig. 1B; see also Fig. S1 in the supplemental material).

To analyze exon 7 splicing in these cells, we used well-established minigene reporters (30) that express the region between exon 6 and exon 8 of either *SMN1* or *SMN2* genes under the control of the CMV promoter (see Fig. S2A in the supplemental material). RT-PCR analysis of *SMN1* and *SMN2* minigenes tran-

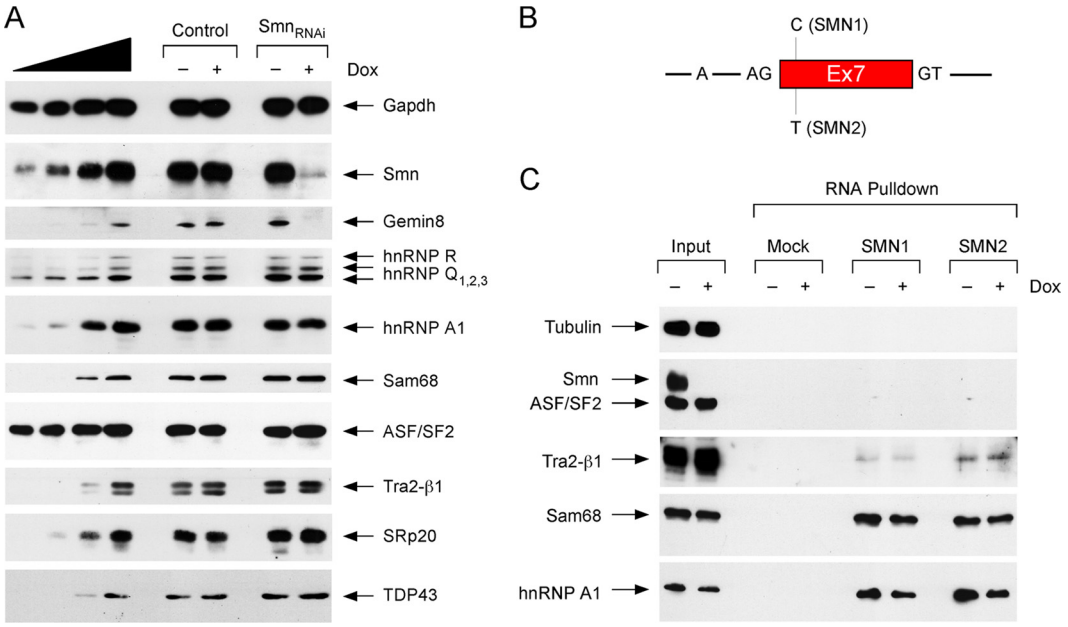

FIG 2 SMN deficiency has no effects on *trans*-acting regulators of exon 7 splicing. (A) Western blot analysis of wild-type (Control) and NIH 3T3-Smn$_{RNAi}$ cells cultured for 5 days without (−) or with (+) Dox. Blots were probed with antibodies against proteins that have been previously implicated in the regulation of SMN exon 7 splicing. Increasing amounts of protein extract from wild-type NIH 3T3 cells (12.5%, 25%, 50%, and 100%, respectively) were loaded on the left side of the blot as a reference for protein quantification. Gemin8 was used as positive control for a protein whose expression is affected by SMN deficiency (11) and GAPDH as a loading control. (B) Schematic representation of the *SMN1* and *SMN2* RNA probes used in pulldown assays. The probes encompass the last 68 nucleotides of SMN intron 6, the entire exon 7, and the first 25 nucleotides of intron 7. The nucleotide difference between the *SMN1* (C) and *SMN2* (T) RNAs as well as the splice junctions (GT and AG) and the branch point adenosine (A) are indicated. (C) Biotinylated RNA probes (*SMN1* and *SMN2*) or no RNA probe (mock) were incubated with whole-cell extracts from NIH 3T3-Smn$_{RNAi}$ cells grown in culture for 5 days without (−) or with (+) Dox. RNA-protein complexes were purified on streptavidin agarose, and bound proteins were analyzed by Western blotting with the indicated antibodies. Input represents 10% of the total amount of protein extract used in the assay.

siently transfected in wild-type NIH 3T3 cells showed the expected alternatively spliced products corresponding to SMN mRNAs that either contain or lack exon 7 (see Fig. S2B). No RT-PCR products were observed following transfection of an empty vector (mock). Quantification of multiple transfection experiments indicates that exon 7 is included in ~80% of *SMN1* mRNAs and ~6% of *SMN2* mRNAs in NIH 3T3 (see Fig. S2C). Thus, transfected NIH 3T3 fibroblasts display a pattern of exon 7 splicing similar to that of endogenous *SMN1* and *SMN2* genes in human cells.

We then asked whether SMN levels affect splicing of exon 7 in human *SMN1* and *SMN2* mRNAs. Strikingly, RT-PCR analysis following transient transfection of splicing reporters in NIH 3T3-Smn$_{RNAi}$ cells depleted of endogenous Smn demonstrates that the efficiency of exon 7 inclusion in both *SMN1* (without Dox, 83.6% ± 2.7%; with Dox, 55.5% ± 3.8%; $P < 0.001$) and *SMN2* (without Dox, 6.4% ± 1.1%; with Dox, 3.1% ± 0.7%; $P < 0.05$) mRNAs was strongly reduced compared to the same cells with normal SMN levels (Fig. 1C and D). Importantly, we found no significant differences in exon 7 splicing for both SMN1 (without Dox, 76.2% ± 2%; with Dox, 77.3% ± 0.2%) and SMN2 (without Dox, 5.5% ± 0.1%; with Dox, 5.6% ± 0.2%) mRNAs in NIH 3T3-SMN/Smn$_{RNAi}$ cells with or without endogenous Smn, indicating that expression of human SMN restored the normal pattern of exon 7 splicing (Fig. 1E and F). Therefore, the observed changes in exon 7 splicing are direct and specific consequences of SMN dysfunction. Moreover, since depletion of SMN impairs exon 7 inclusion in both *SMN1* and *SMN2* mRNAs to similar extents, the SMN-dependent effect on exon 7 splicing appears to be independent of the C-to-T transition. These results demonstrate that deficiency of SMN protein affects the splicing of its own mRNA through a negative feedback loop that decreases inclusion of exon 7.

SMN deficiency does not affect known regulators of exon 7 splicing. Several *trans*-acting factors have been implicated in the regulation of SMN exon 7 splicing (5, 51, 58). To investigate the mechanism by which SMN regulates its own splicing, we first tested the possibility that SMN depletion may influence the expression of these known regulators of exon 7 splicing which, in turn, would lead to inhibition of exon 7 inclusion. To do so, we carried out Western blot analysis of NIH 3T3-Smn$_{RNAi}$ cells cultured in the absence or presence of doxycycline for 5 days as well as wild-type NIH 3T3 cells as a control (Fig. 2A; see also Fig. S3 in the supplemental material). Consistent with previous studies (11, 22, 64), the expression of Gemin8—a core component of the SMN complex (11)—was strongly reduced upon SMN depletion, while doxycycline treatment had no effect in wild-type cells. Interestingly, we found that the expression levels of all known regulators of *SMN2* exon 7, including several members of the hnRNP and SR protein families, were unchanged in Smn-deficient NIH 3T3 fibroblasts (Fig. 2A; see also Fig. S3).

Even though SMN deficiency does not appear to affect the expression of known splicing regulators of exon 7, it is possible that low SMN levels could influence the subcellular localization of these proteins or their association with SMN pre-mRNA. Immunofluorescence analysis showed that the predominantly nuclear localization of *trans*-acting factors involved in exon 7 splicing reg-

ulation does not change in SMN-deficient NIH 3T3 cells (see Fig. S4 in the supplemental material). To investigate potential changes in the association with SMN pre-mRNA, we carried out pulldown experiments from NIH 3T3 extracts using biotinylated *SMN1* and *SMN2* RNAs comprising SMN exon 7 and a short portion of flanking introns, including splice sites and the branch point adenosine (Fig. 2B). These RNAs were incubated with whole-cell extracts from control and Smn-deficient NIH 3T3-Smn_{RNAi} cells, and following capture on streptavidin beads and extensive washing, bound proteins were analyzed by Western blotting. Known regulators of exon 7 splicing such as Tra2-β1, Sam68, and hnRNP A1 could be specifically isolated, but their binding to either *SMN1* or *SMN2* RNAs was not affected by SMN deficiency (Fig. 2C). Significant association of other putative *trans*-acting regulators of exon 7 splicing as well as SMN binding to its own mRNA was not detected (Fig. 2C). Taken together, these results show that the effects of SMN deficiency on exon 7 inclusion are unlikely to be mediated by changes in the expression, subcellular localization, or function of *trans*-acting splicing factors.

Defective snRNP biogenesis decreases exon 7 inclusion in SMN mRNAs. SMN has a well-established function in the assembly of spliceosomal snRNPs that are essential for pre-mRNA splicing (15, 52), and SMN deficiency decreases snRNP levels in NIH 3T3 fibroblasts (Fig. 1; see also Fig. S1 in the supplemental material) as well as tissues of SMA mice (22, 64). These observations raise the possibility that altered snRNP levels may mediate the effects of SMN deficiency on exon 7 splicing. To address this, we analyzed the consequences on exon 7 splicing of specifically disrupting the pathway of snRNP biogenesis without perturbing SMN levels. To do so, we generated a stable NIH 3T3 cell line (NIH 3T3-SmB_{RNAi}) with doxycycline-inducible, RNAi-mediated knockdown of SmB—a core snRNP component (61)—using a lentiviral vector expressing an shRNA targeting endogenous mouse SmB mRNA. Western blot analysis of NIH 3T3-SmB_{RNAi} cells demonstrates specific reduction of endogenous SmB upon addition of doxycycline to the medium without any changes in SMN levels (Fig. 3A). Next, we analyzed the effect of SmB deficiency on SMN-dependent snRNP assembly. To do so, we used a well-established *in vitro* assay that monitors Sm core formation on radioactive U1 snRNA by gel shift (54) with three increasing amounts of extract from either control or SmB-deficient NIH 3T3 cells (Fig. 3B). This analysis demonstrated that SmB deficiency strongly impairs snRNP assembly. Thus, in these cells the same molecular defect triggered by SMN deficiency—disruption of the snRNP biogenesis pathway—is accomplished in the presence of normal SMN expression levels.

To test whether dysfunction in snRNP biogenesis affects exon 7 splicing, *SMN1* and *SMN2* splicing reporters were transfected in control and SmB-deficient NIH 3T3 cells. RT-PCR analysis shows that SmB deficiency causes a strong decrease in the efficiency of exon 7 inclusion in both *SMN1* (without Dox, 86.3% $\pm$ 2.5%; with Dox, 44.2% $\pm$ 2%; $P < 0.001$) and *SMN2* (without Dox, 6% $\pm$ 0.3%; with Dox, 2.3% $\pm$ 0.4%; $P < 0.01$) mRNAs (Fig. 3C and D). These results indicate that SmB-dependent impairment of snRNP assembly affects SMN exon 7 splicing in a manner similar to that of SMN deficiency and that the observed changes in exon 7 splicing regulation likely occur through snRNP-dependent mechanisms.

Motor neurons express lower levels of full-length *SMN2* mRNA than do dorsal horn cells in the spinal cord. We next sought to investigate the regulation of SMN exon 7 splicing *in vivo* in motor neurons from control and SMA mice. To do so, we relied on laser capture microdissection (LCM) of cells from specific areas of the lumbar spinal cord (Fig. 4A). In addition to motor neurons (MNs) in the ventral horn, we collected cells located in the dorsal horn of the same spinal segment as a control. This area of the spinal cord contains a mixture of glia and neurons but is devoid of motor neurons (here collectively referred to as non-MNs). For these studies, we used spinal cords isolated from *SMN2*-expressing carrier (*Smn*$^{+/-}$; *SMN2*$^{+/+}$; SMNΔ7$^{+/+}$; GFP$^{+/-}$) and Δ7 SMA (*Smn*$^{-/-}$; *SMN2*$^{+/+}$; SMNΔ7$^{+/+}$; GFP$^{+/-}$) mice. In addition to two copies of the human *SMN2* gene, these mice contain several transgenic copies of the SMNΔ7 cDNA and express GFP under the control of the motor neuron-specific Hb9 promoter (32, 42). Compared to mice with only two copies of the *SMN2* gene, which survive up to 4 days (46), the presence of the SMNΔ7 transgenes extends the life span of SMA mice to 14 days (32). The Δ7 SMA mouse is the best-characterized and most widely used model of SMA for the study of disease mechanisms as well as preclinical therapy development (8, 49).

First, we designed and experimentally validated a set of primers ($SMN2_{TOT}$) that would allow us to measure by RT-qPCR the total levels of human SMN mRNAs (both FL and Δ7) specifically transcribed from the *SMN2* gene but not those from the SMNΔ7 transgene (see Fig. S5 in the supplemental material). To do so, we took advantage of the fact that the SMNΔ7 transgene lacks the terminal part of the 3′ untranslated region of the human *SMN2* gene (see Fig. S5A). This primer pair ($SMN2_{TOT}$) and a second set of primers (SMN)—complementary to a region in exon 6 shared by both the *SMN2* gene and the SMNΔ7 transgene—were used in RT-qPCR experiments with total RNA from the spinal cord of control (*Smn*$^{+/+}$; *SMN2*$^{+/+}$), SMA (*Smn*$^{-/-}$; *SMN2*$^{+/+}$), and Δ7 SMA (*Smn*$^{-/-}$; *SMN2*$^{+/+}$; SMNΔ7$^{+/+}$) mice. According to the genotype, analysis with primers specific for mouse Smn showed no expression of mouse Smn mRNA in samples from SMA and Δ7 SMA mice (see Fig. S5B). The SMN-specific primer set detected approximately 9-fold more human SMN mRNA in Δ7 SMA mice than in control and SMA mice (see Fig. S5C). The increase in SMN mRNA levels in Δ7 SMA animals is consistent with the presence of several SMNΔ7 transgene copies in these animals. In contrast, $SMN2_{TOT}$ primers detected the same levels of human SMN mRNA in all mice (see Fig. S5D). The fact that higher RNA levels in Δ7 SMA are not detected when using $SMN2_{TOT}$ primers indicates that these primers specifically monitor the mRNA transcribed from the *SMN2* gene and not those coming from the SMNΔ7 transgenes. Finally, both SMN and $SMN2_{TOT}$ primer sets are human specific, as they detect similar levels of SMN mRNA in control and SMA mice both in the presence and in the absence of mouse Smn alleles. Thus, we developed an assay that allows us to measure SMN mRNAs transcribed specifically from the *SMN2* gene in SMA mice containing high copy numbers of the SMNΔ7 transgene and that will be useful for future studies in Δ7 SMA mice.

Using this assay, we then carried out RT-qPCR analysis of RNA isolated from LCM MNs and LCM non-MNs of the spinal cord of normal mice (*Smn*$^{+/-}$; *SMN2*$^{+/+}$; SMNΔ7$^{+/+}$; GFP$^{+/-}$). Similar levels of mRNA expression in MNs and non-MNs of another housekeeping gene, Atp6, relative to GAPDH support the use of the latter as an appropriate normalizer between different cell populations (Fig. 4B). Importantly, mRNAs for the motor neuron

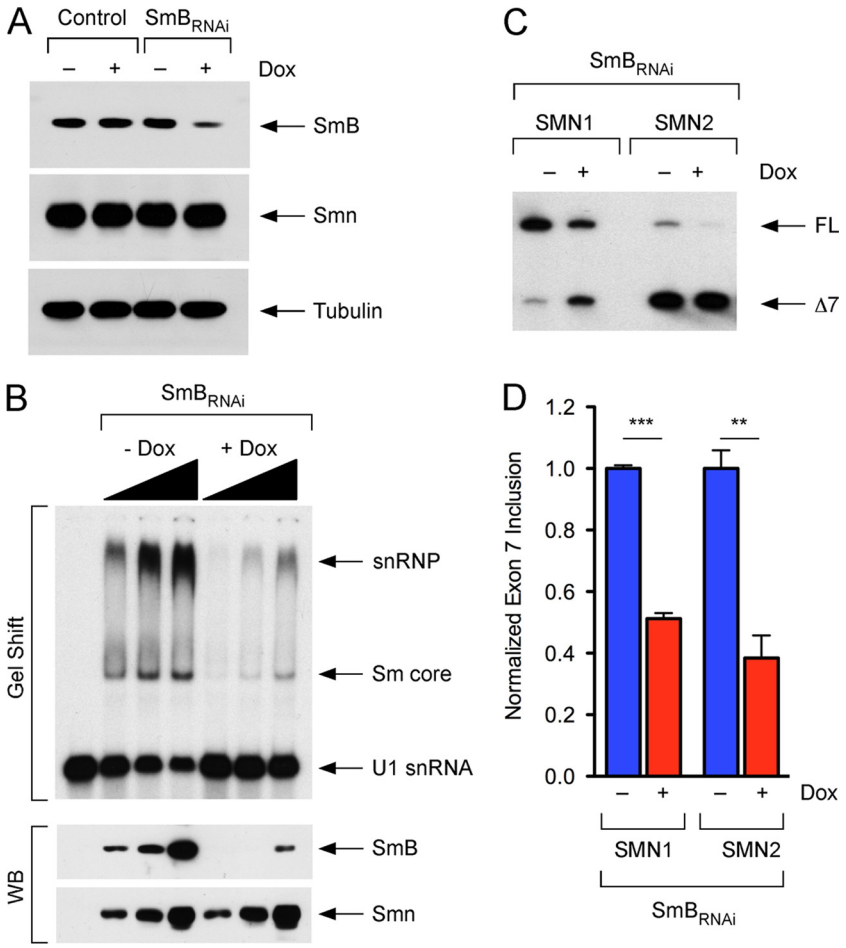

FIG 3 SmB deficiency impairs snRNP assembly and exon 7 splicing. (A) NIH 3T3 cell lines with regulated knockdown of mouse SmB. Western blot analysis of NIH 3T3 wild-type (Control) and NIH 3T3-SmB$_{RNAi}$ cells cultured for 4 days without (−) or with (+) Dox. Blots were probed with antibodies against SmB to monitor knockdown efficiency and tubulin as a loading control. Note that SMN expression is not decreased by SmB deficiency. (B) SmB deficiency impairs snRNP assembly in NIH 3T3 cells. Three increasing amounts of extracts from NIH 3T3-SmB$_{RNAi}$ cells (10 μg, 20 μg, and 40 μg) cultured for 5 days without (−) or with (+) Dox were analyzed by *in vitro* snRNP assembly with radioactive U1 snRNA. Reaction mixtures were analyzed by gel shift, and known RNA-protein complexes are indicated on the right (top panel) (54). SmB and SMN protein levels in the extracts used for snRNP assembly were analyzed by Western blotting (bottom panels). (C) SmB deficiency decreases the efficiency of exon 7 inclusion in NIH 3T3 cells. Radioactive RT-PCR analysis of exon 7 splicing following transfection of *SMN1* or *SMN2* minigene reporters into NIH 3T3-SmB$_{RNAi}$ cells cultured without (−) or with (+) Dox. Arrows point to exon 7-included (FL) and exon 7-skipped (Δ7) SMN mRNAs. (D) Quantification of the efficiency of exon 7 inclusion in NIH 3T3-SmB$_{RNAi}$. Blue and red bars correspond to results from NIH 3T3 cells cultured without (−) or with (+) Dox, respectively. Values represent means and SEM from independent experiments ($n = 3$; **, $P < 0.01$; ***, $P < 0.001$) as in panel C. Data were normalized relative to −Dox set as 1.

markers ChAT and GFP were expressed at 50- and 150-fold-higher levels in MNs than in non-MNs, respectively (Fig. 4B), demonstrating very strong enrichment of motor neurons by LCM. We then analyzed the expression levels of total (SMN2$_{TOT}$) and full-length (SMN2$_{FL}$) SMN mRNAs specifically transcribed from the *SMN2* gene in MNs and non-MNs of normal mice. Strikingly, while total *SMN2* mRNA levels did not significantly differ between the two cell populations, MNs expressed 75% less full-length *SMN2* mRNA ($P < 0.01$) than did non-MNs from the same lumbar spinal segment (Fig. 4C). To analyze the mechanism for this remarkable difference, we measured the relative efficiency of exon 7 inclusion in MNs and non-MNs from normal mice following normalization to total *SMN2* mRNA levels. Figure 4D shows that exon 7 inclusion is 65% less efficient in MNs than in non-MNs ($P < 0.05$). Altogether, these results indicate that normal motor neurons are remarkably inefficient in their ability to include exon 7 in *SMN2* mRNAs and that this splicing difference likely accounts for a 4-fold reduction in the steady-state levels of full-length *SMN2* mRNA compared to other cells in the spinal cord.

SMN deficiency impairs exon 7 inclusion in SMA motor neurons. To determine the effect of SMN deficiency on exon 7 splicing in SMA mice, we carried out RT-qPCR experiments with total RNA from spinal cord as well as LCM MNs and non-MNs from control (*Smn*$^{+/-}$; *SMN2*$^{+/+}$; SMNΔ7$^{+/+}$; GFP$^{+/-}$) and Δ7 SMA (*Smn*$^{-/-}$; *SMN2*$^{+/+}$; SMNΔ7$^{+/+}$; GFP$^{+/-}$) mice. Analysis of the whole spinal cord revealed no differences in the efficiency of *SMN2* exon 7 splicing between control and Δ7 SMA animals (Fig. 5A). Similar results were obtained by semiquantitative RT-PCR as well as RT-qPCR analysis of control (*Smn*$^{+/+}$; *SMN2*$^{+/+}$) and SMA (*Smn*$^{-/-}$; *SMN2*$^{+/+}$) spinal cords from a different mouse model of SMA (46) lacking the SMNΔ7 transgene (see Fig. S6 in

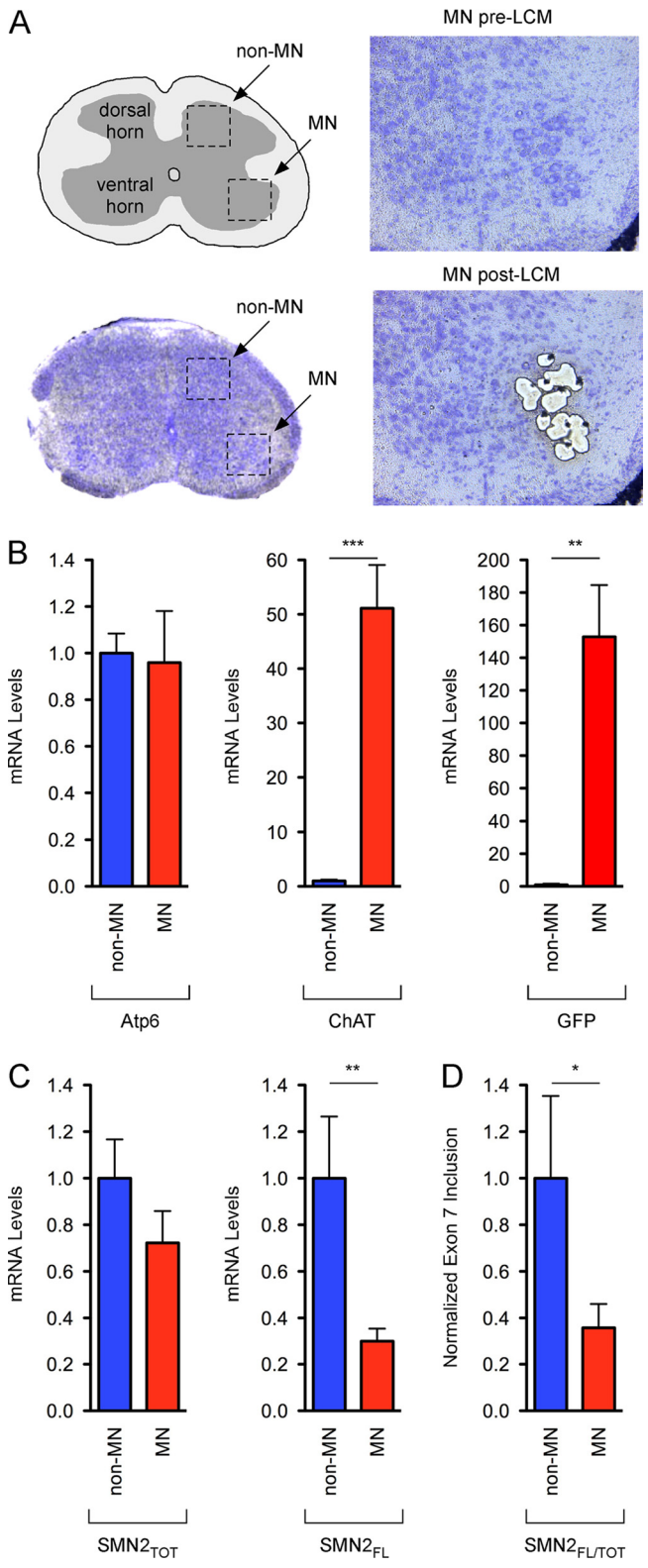

FIG 4 Normal motor neurons express remarkably lower levels of full-length *SMN2* mRNA than non-motor neurons due to inefficient exon 7 splicing. (A) Schematic representation (top left) and Nissl-stained image (bottom left) of a transverse section of the mouse spinal cord. Nissl-stained images of the ventral horn area of the spinal cord before (top right) and after (bottom right) laser capture microdissection (LCM) of motor neurons are shown. (B) Validation of LCM motor neurons. Real-time RT-qPCR analysis of the expression of Atp6, ChAT, and GFP mRNAs relative to GAPDH mRNA in LCM motor neurons (MNs) and LCM non-motor neurons (non-MNs) from the spinal cord of normal mice ($Smn^{+/-}$; $SMN2^{+/+}$; SMN$\Delta7^{+/+}$; GFP$^{+/-}$) at postnatal day 6. (C) Normal motor neurons express much less full-length *SMN2* mRNA than do non-motor neurons. Real-time RT-qPCR analysis of the expression of total (FL+Δ7; $SMN2_{TOT}$) and full-length (FL; $SMN2_{FL}$) *SMN2* mRNAs relative to GAPDH mRNA in LCM MNs and LCM non-MNs. (D) Exon 7 inclusion is less efficient in normal motor neurons than in non-motor neurons. Normalized exon 7 inclusion was measured by real-time RT-qPCR analysis of the expression of full-length ($SMN2_{FL}$) relative to total ($SMN2_{TOT}$) *SMN2* mRNAs in LCM MNs and LCM non-MNs. Values represent means and SEM from independent experiments ($n = 8$; *, $P < 0.05$; **, $P < 0.01$; ***, $P < 0.001$).

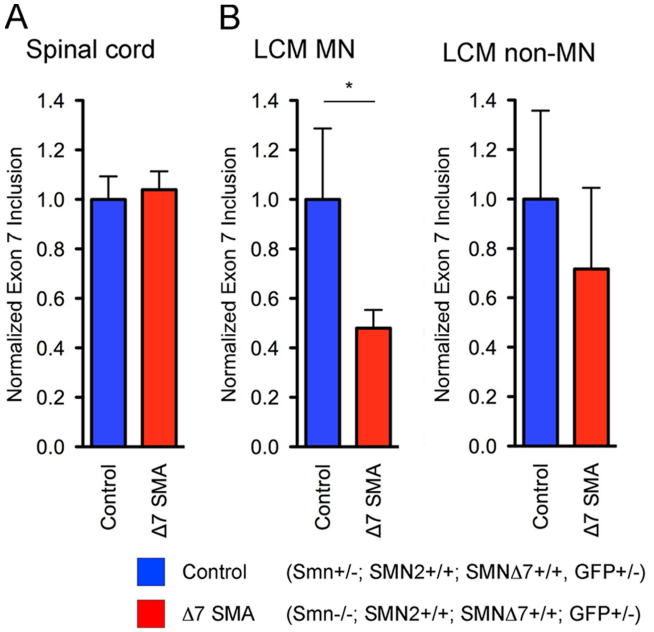

FIG 5 SMN deficiency impairs exon 7 splicing in SMA motor neurons. Analysis of the relative efficiency of exon 7 inclusion in the whole spinal cord (A) as well as motor neurons (LCM MNs) and non-motor neurons (LCM non-MNs) (B) isolated from control ($Smn^{+/-}$; $SMN2^{+/+}$; SMN$\Delta7^{+/+}$; GFP$^{+/-}$) and $\Delta7$ SMA ($Smn^{-/-}$; $SMN2^{+/+}$; SMN$\Delta7^{+/+}$; GFP$^{+/-}$) mice at postnatal day 6. Normalized exon 7 inclusion was measured by real-time RT-qPCR analysis of the expression of full-length ($SMN2_{FL}$) relative to total ($SMN2_{TOT}$) *SMN2* mRNAs. Values represent means and SEM from independent experiments ($n = 8$; *, $P < 0.05$).

the supplemental material). Thus, SMN deficiency does not affect exon 7 inclusion generally in neural tissue of SMA mice. In contrast, motor neurons in the lumbar spinal cord of $\Delta7$ SMA mice included ~50% less exon 7 ($P < 0.05$) than did normal motor neurons (Fig. 5B). Despite greater experimental variability, likely due to the heterogeneity of cells in the dorsal horn region, no significant difference in the efficiency of exon 7 splicing was observed between non-MNs from control mice and those from $\Delta7$ SMA mice (Fig. 5B), which is also consistent with results in whole spinal cord tissue. These results show that SMN protein deficiency decreases *SMN2* exon 7 inclusion in motor neurons *in vivo* and that this effect appears to be specific for the most vulnerable cell type in SMA.

Downstream effects of SMN deficiency are exacerbated in SMA motor neurons. Further reduction in exon 7 inclusion,

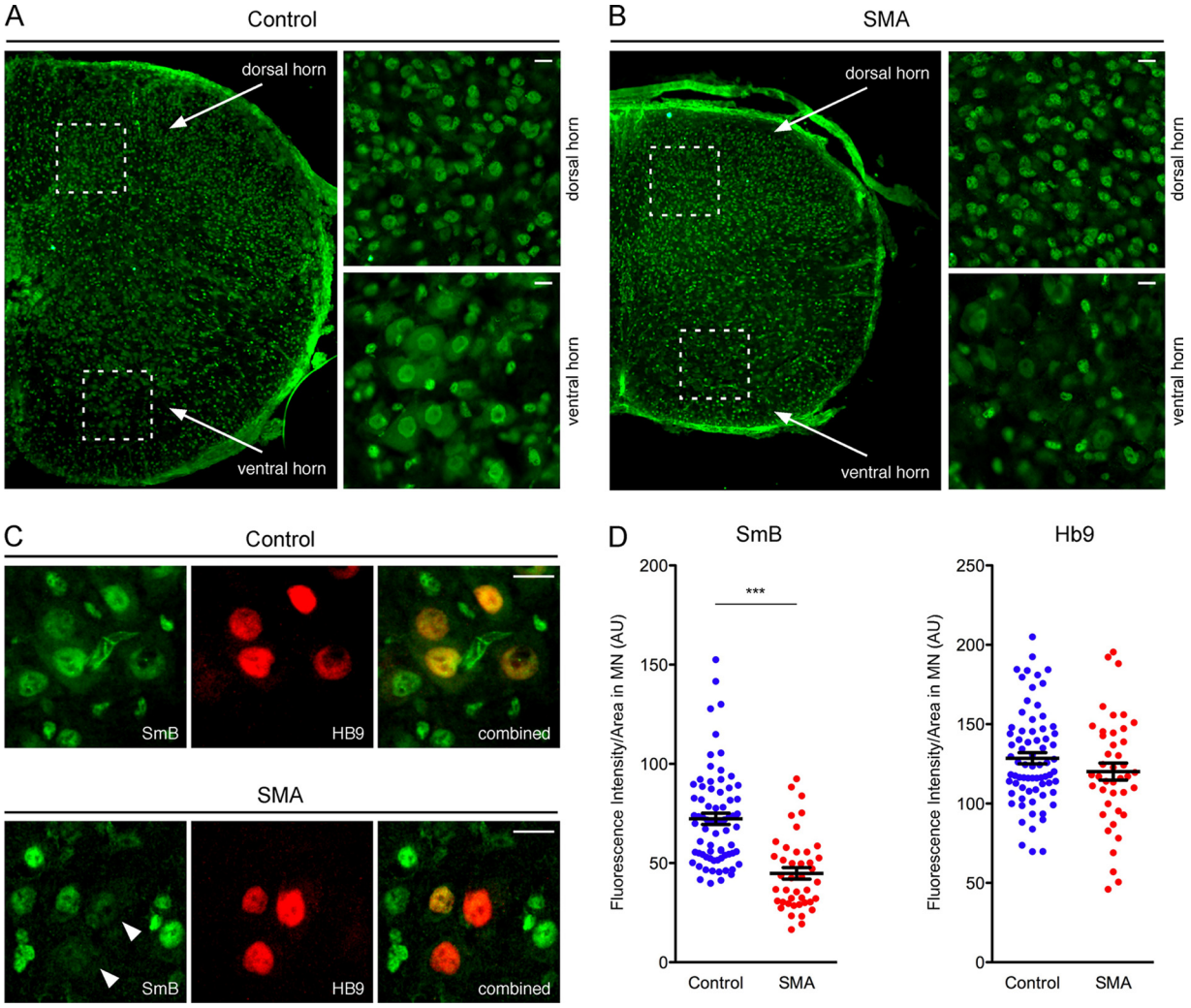

FIG 6 SMN deficiency decreases nuclear levels of SmB protein in SMA motor neurons. (A) Immunohistochemistry analysis with anti-SmB antibodies of a spinal cord section from control (*Smn*$^{+/+}$; *SMN2*$^{+/+}$; SMNΔ7$^{+/+}$) mouse at postnatal day 10. Higher-magnification images of dorsal and ventral horn regions are shown on the right. Note the strong ubiquitous nuclear SmB immunoreactivity as well as detectable staining of the cytoplasm in large ventral horn cells that are likely motor neurons. Bars, 10 μm. (B) Immunohistochemistry analysis with anti-SmB antibodies of a spinal cord section from Δ7 SMA (*Smn*$^{-/-}$; *SMN2*$^{+/+}$; SMNΔ7$^{+/+}$) mouse at postnatal day 10. Higher-magnification images of dorsal and ventral horn regions are shown on the right. There is a reduction in SmB staining of large ventral horn cells from SMA mice compared to control mice. Bars, 10 μm. (C) Analysis by double-label immunofluorescence and confocal microscopy of spinal cord sections from control (*Smn*$^{+/+}$; *SMN2*$^{+/+}$; SMNΔ7$^{+/+}$) and Δ7 SMA (*Smn*$^{-/-}$; *SMN2*$^{+/+}$; SMNΔ7$^{+/+}$) mice at postnatal day 10 with anti-SmB and anti-Hb9 antibodies. Arrowheads point to SMA motor neurons with strongly reduced SmB levels. Bars, 10 μm. (D) Quantification of SmB and Hb9 expression in the nucleus of motor neurons. Each data point represents the average fluorescence intensity per unit area in individual Hb9^{+} nuclei from control ($n = 72$) and SMA ($n = 42$) motor neurons measured from confocal images as in panel C. Means and SEM are shown (***, $P < 0.001$).

combined with the already lower levels of full-length *SMN2* mRNA under normal conditions, would be expected to exacerbate the downstream effects of SMN deficiency in SMA motor neurons. To investigate this possibility, we sought to measure the degree of SMN-dependent changes in the expression of downstream targets as a readout of SMN dysfunction in different cell types of the spinal cord. We first looked at changes in the levels of spliceosomal snRNPs that are well-established targets of SMN function affected in SMA (22, 64). Reduced nuclear accumulation of Sm proteins has previously been used as a measure of snRNP biogenesis defects *in situ* in the mouse spinal cord (28). Our immunohistochemical analysis with antibodies against the snRNP core component SmB revealed the expected widespread expression in the spinal cord of normal mice and predominant localization in the nucleus (Fig. 6A). Despite a remarkable difference in tissue size, SmB expression levels appeared overall similar in the spinal cord of control (*Smn*$^{+/+}$; *SMN2*$^{+/+}$; SMNΔ7$^{+/+}$) and Δ7 SMA (*Smn*$^{-/-}$; *SMN2*$^{+/+}$; SMNΔ7$^{+/+}$) mice (Fig. 6A and B). This is consistent with the relatively modest reduction of snRNP levels in SMA mice (22, 64). However, SmB immunoreactivity of large ventral horn cells appeared strongly decreased in Δ7 SMA mice compared to normal mice, while no differences among other ventral horn cells or dorsal horn cells were evident (Fig. 6A and B). To determine whether these large ventral horn cells were motor neurons as suggested by their location and size, we carried out double labeling experiments with antibodies against SmB and the motor neuron-specific marker Hb9 (1), followed by quantification of expression levels of these proteins in the nucleus of motor

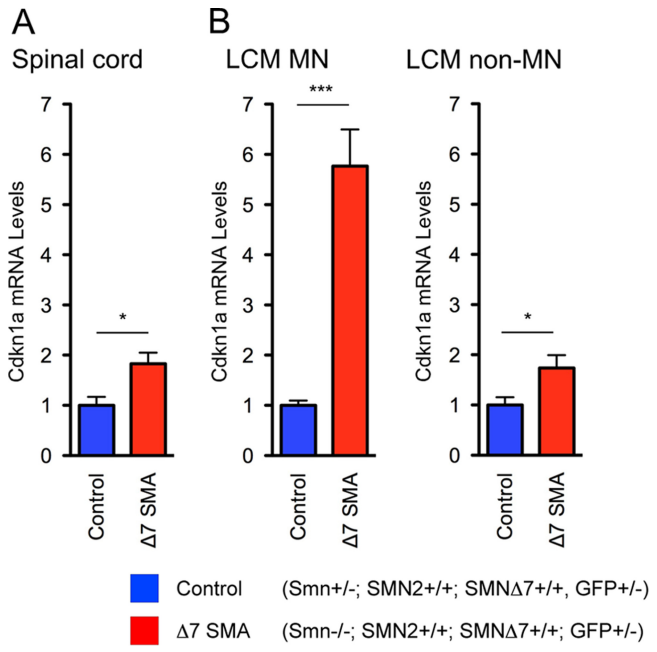

FIG 7 SMN deficiency exacerbates Cdkn1a mRNA upregulation in SMA motor neurons. RT-qPCR analysis of Cdkn1a mRNA expression in whole spinal cord (A) as well as motor neurons (LCM MN) and non-motor neurons (LCM non-MN) (B) isolated from control (*Smn*$^{+/-}$; *SMN2*$^{+/+}$; SMNΔ7$^{+/+}$; GFP$^{+/-}$) and Δ7 SMA (*Smn*$^{-/-}$; *SMN2*$^{+/+}$; SMNΔ7$^{+/+}$; GFP$^{+/-}$) mice at postnatal day 6. Data were normalized to GAPDH, and for each group, Cdkn1a mRNA levels in Δ7 SMA were expressed relative to those in control. Values represent means and SEM from independent experiments ($n = 8$; *, $P < 0.05$; ***, $P < 0.001$).

neurons (Fig. 6C and D). These experiments showed that SMN deficiency causes an average 40% decrease ($P < 0.001$) in the levels of SmB expression in SMA motor neurons. This reduction is specific because similar levels of Hb9 expression were found in motor neurons of normal and Δ7 SMA mice.

Next, we analyzed changes in the expression of the cyclin-dependent kinase inhibitor 1A (Cdkn1a) mRNA—a negative regulator of the cell cycle also known as p21, Cip1, or Waf1. Previous studies have identified upregulation of Cdkn1a mRNA as a specific downstream effect of SMN deficiency that occurs in tissues from human SMA patients and mouse models (4, 20, 48, 64). This event is mediated by an increase in the stability of Cdkn1a mRNA that is dependent on the activity of two RNA-binding proteins—HuD and KSRP (KH-type splicing regulatory protein)—which interact with SMN and are dysregulated in SMA (7, 24, 27, 59). Consistent with previous studies, we found a significant 1.8-fold ($P < 0.05$) increase in Cdkn1a mRNA levels in the spinal cord of Δ7 SMA mice compared to unaffected controls (Fig. 7A). Strikingly, LCM SMA motor neurons displayed a 6-fold ($P < 0.001$) increase in Cdkn1a mRNA expression, while the increase in SMA non-MNs (1.7-fold; $P < 0.05$) is similar to that found in whole spinal cord (Fig. 7B). Altogether, our results provide direct evidence that these downstream defects triggered by SMN deficiency are more prominent in motor neurons than in other spinal cord cells in SMA mice.

DISCUSSION

The basis for the selective vulnerability of motor neurons to reduced SMN expression has proven elusive despite progress in our basic understanding of SMA biology. To investigate whether cell type-specific features of SMN gene expression contribute to motor neuron vulnerability in SMA, we looked for differences in the regulation of SMN exon 7 splicing *in vivo*. We show that normal motor neurons express markedly lower levels of full-length SMN mRNA from the *SMN2* gene than do other cells in the spinal cord. This is due to the particularly low efficiency of exon 7 splicing that characterizes motor neurons even under normal conditions. Through studies of loss of SMN function in cellular and animal models, we also show that severe SMN deficiency triggers a negative feedback loop leading to decreased exon 7 inclusion. Importantly, this mechanism is active *in vivo* and further decreases *SMN2* exon 7 splicing specifically in SMA motor neurons. Consistent with expression of lower levels of full-length SMN in motor neurons, we provide evidence that downstream molecular defects caused by SMN deficiency are more prominent in motor neurons than in other spinal cells from SMA mice. Based on our data, we propose that one reason that motor neurons are preferentially vulnerable to loss of *SMN1* is because they express less functional SMN from the *SMN2* gene than do other cell types.

One of the most important findings of our work came from comparison of *SMN2* gene expression levels in motor neurons and other cells in the spinal cord of normal mice. We discovered that motor neurons express 4-fold less full-length *SMN2* mRNA than do dorsal horn cells from the same spinal segment. This striking difference is due to changes not in *SMN2* gene transcription but in the efficiency of exon 7 inclusion in *SMN2* mRNAs. Since inclusion of exon 7 is essential for the stability of the SMN protein (9, 18, 36), this would result in a greater reduction of functional SMN in SMA motor neurons. A 4-fold difference in the levels of full-length *SMN2* mRNA can be critical for motor neuron biology and underlie dysfunction of this disease-relevant neural type upon loss of *SMN1*. Consistent with this conclusion, studies in mouse models showed that two copies of the *SMN2* gene produce enough full-length SMN for normal function of most cells except motor neurons causing SMA, whereas eight *SMN2* gene copies fully rescue the SMA phenotype (46). This is also in agreement with *SMN2* gene copy number being the main disease modifier in human SMA patients (8, 44).

Our analysis in SMA mice identified *SMN2* exon 7 inclusion as an SMN-dependent splicing event that is affected in motor neurons and might contribute to SMA pathology. Early studies showed that the ratio of *SMN2* exon 7 inclusion is high in lymphoblasts from mild SMA patients and low in those from severe SMA patients (23, 26), highlighting an inverse correlation of clinical severity with the efficiency of *SMN2* exon 7 inclusion. We therefore investigated the effects of SMN deficiency on the splicing of its own mRNA and links of this feedback circuitry with SMA pathology. We found a 2-fold decrease in the efficiency of *SMN2* exon 7 inclusion in SMA motor neurons compared to control motor neurons. In contrast, we found no significant effect of SMN deficiency on exon 7 splicing in either dorsal horn cells or whole spinal cord. Our findings are in contrast to a recent report showing decreased exon 7 inclusion in the spinal cord of SMA mice (29). Although the reason for this discrepancy is unclear, we note that the previous study limited the analysis to tissue from a single animal per genotype (29), while here we analyzed the spinal cord of two distinct mouse models of severe SMA using at least three animals per group and two distinct techniques. Collectively, our findings indicate that SMN deficiency decreases exon 7 inclusion

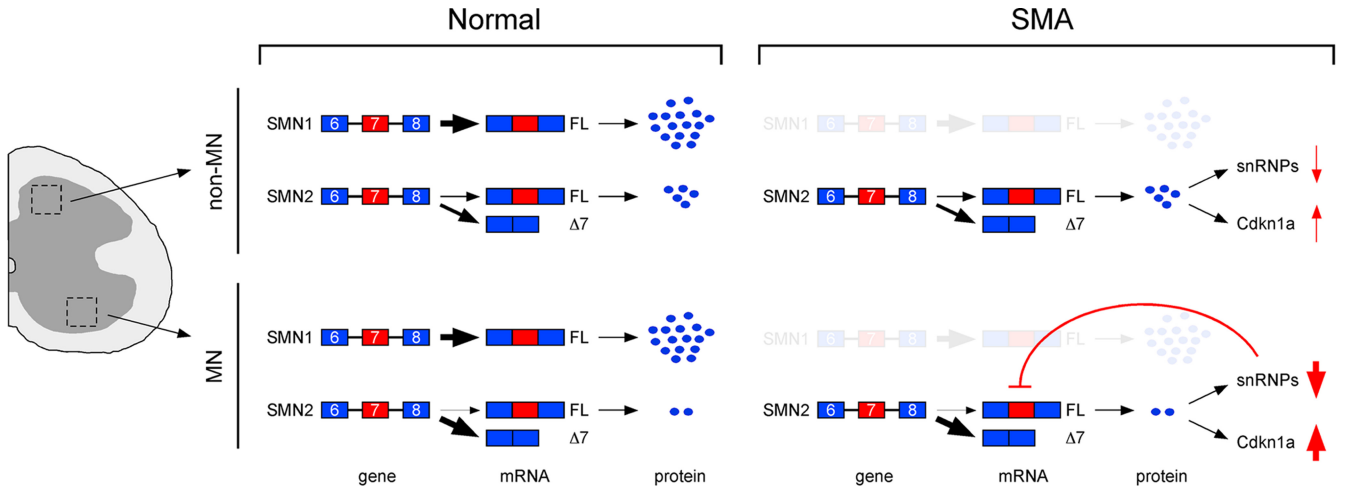

FIG 8 Model for the selective vulnerability of motor neurons in SMA. Under normal conditions, the *SMN2* gene produces smaller amounts of full-length SMN mRNA and protein in motor neurons (MN) than in non-motor neurons (non-MN) due to more inefficient exon 7 splicing. Upon loss of the protective *SMN1* allele, the downstream effects of SMN deficiency in SMA MNs are exacerbated compared to non-MNs due to the lower SMN levels. These include downregulation of nuclear snRNP levels and upregulation of Cdkn1a mRNA expression. Moreover, reduced snRNP levels trigger a negative feedback loop affecting exon 7 splicing that might contribute to further decreasing SMN expression and enhancing downstream defects specifically in SMA MNs.

specifically in motor neurons but not generally in the spinal cord of SMA mice, consistent with the presence of a threshold of SMN reduction that needs to be reached to affect exon 7 splicing *in vivo*. One reason that this threshold might be reached in SMA motor neurons and not in other spinal cells is the lower levels of functional SMN expressed from SMN2 in motor neurons under normal conditions. This situation would bring about a further reduction in the levels of full-length SMN2 mRNA that might enhance the downstream effects of SMN deficiency specifically in SMA motor neurons.

Our results indicate that SMN deficiency decreases exon 7 splicing through a negative feedback loop activated by disruption of SMN function in snRNP biogenesis. We found that SMN depletion caused a strong decrease in exon 7 inclusion in NIH 3T3 cells. However, this effect appears to be independent of the *cis*-acting elements and *trans*-acting factors that regulate exon 7 splicing (5, 51, 58). Low SMN levels decreased exon 7 inclusion of both *SMN1* and *SMN2* mRNAs to similar extents and did not change the expression or subcellular localization of known regulators of exon 7 splicing as well as their ability to associate with SMN pre-mRNA. Conversely, SMN deficiency decreased the levels of spliceosomal snRNPs, and these changes coincide with reduced exon 7 splicing in both NIH 3T3 fibroblasts and SMA motor neurons. Since exon 7 inclusion may be particularly sensitive to SMN-dependent changes in snRNP abundance due to the presence of suboptimal splice site signals flanking exon 7 (39, 57), we investigated the link between impaired snRNP biogenesis and decreased exon 7 splicing. We found that SmB knockdown in NIH 3T3 cells—which disrupted snRNP assembly without changing SMN levels—caused a reduction in exon 7 splicing remarkably similar to that observed when SMN is depleted. Our findings, together with those of a recent study (29), support the conclusion that SMN-dependent effects on exon 7 splicing are mediated by a decrease in snRNP levels and that the negative feedback loop triggered by SMN deficiency is activated by impairment of its critical function in snRNP assembly. This mechanism likely contributes to decrease the efficiency of exon 7 inclusion in SMA motor neurons compared to normal motor neurons.

The particularly low levels of full-length *SMN2* mRNA produced by the *SMN2* gene would be expected to exacerbate the downstream effects of SMN deficiency in SMA motor neurons compared to other spinal cord cells upon loss of *SMN1*. Consistent with this, we found that decreased nuclear accumulation of Sm proteins and upregulation of Cdkn1a mRNA levels are more prominent in motor neurons than in other cells in the spinal cord of SMA mice. Thus, using these SMN-dependent events as readouts of the degree of SMN dysfunction in the spinal cord of SMA mice, we provide evidence that molecular defects linked to SMN deficiency are specifically exacerbated in SMA motor neurons.

Based on our findings, we propose a model to explain the long-standing conundrum of the selective vulnerability of motor neurons in SMA (Fig. 8). Normally, the *SMN1* gene produces the vast majority of functional SMN and low levels of full-length SMN are produced from the *SMN2* gene due to its characteristically poor inclusion of exon 7. Under wild-type conditions, cell type-specific differences in the efficiency of *SMN2* exon 7 splicing would have negligible effects on overall SMN levels and thus little physiological relevance. However, the degree of exon 7 inclusion becomes critical upon homozygous loss of the *SMN1* gene (or the *Smn* gene in mouse models), leaving the *SMN2* gene as the only source of functional SMN levels in the organism. According to our model, one reason why SMA motor neurons are selectively vulnerable is because the particularly low efficiency of exon 7 inclusion strongly limits their ability to synthesize full-length SMN from the *SMN2* gene at levels achieved in other spinal cord cells. This would result in a greater reduction in SMN levels and a more prominent dysfunction of SMN-dependent downstream pathways leading to degeneration and loss of motor neurons.

ACKNOWLEDGMENTS

We thank Christopher Henderson and George Mentis for comments and critical reading of the manuscript. We are grateful to James Manley for the

kind gift of *SMN1* and *SMN2* splicing reporter constructs and to Brunhilde Wirth for antibodies against Tra2-β1. We acknowledge the help of Mariangels de Planell Saguer with experiments in Fig. 3.

This work was supported by grants from the Spinal Muscular Atrophy Foundation (to L.P.) and NIH-NINDS R01NS069601 (to L.P.), R01NS057482 (to U.R.M.), and R01NS038650 (to A.H.M.B.). The National Center for Research Resources provided additional funding for LCM work (award no. UL1RR025755 to A.H.M.B.).

The content is solely the responsibility of the authors and does not necessarily represent the official views of the National Center for Research Resources or the National Institutes of Health.

REFERENCES

1. **Arber S, et al.** 1999. Requirement for the homeobox gene Hb9 in the consolidation of motor neuron identity. Neuron **23**:659–674.
2. **Baccon J, Pellizzoni L, Rappsilber J, Mann M, Dreyfuss G.** 2002. Identification and characterization of Gemin7, a novel component of the survival of motor neuron complex. J. Biol. Chem. **277**:31957–31962.
3. **Battle DJ, et al.** 2006. The SMN complex: an assembly machine for RNPs. Cold Spring Harbor Symp. Quant. Biol. **71**:313–320.
4. **Baumer D, et al.** 2009. Alternative splicing events are a late feature of pathology in a mouse model of spinal muscular atrophy. PLoS Genet. **5**:e1000773.
5. **Bebee TW, Gladman JT, Chandler DS.** 2010. Splicing regulation of the survival motor neuron genes and implications for treatment of spinal muscular atrophy. Front. Biosci. **15**:1191–1204.
6. **Bernal S, et al.** 2010. The c.859G>C variant in the SMN2 gene is associated with types II and III SMA and originates from a common ancestor. J. Med. Genet. **47**:640–642.
7. **Briata P, et al.** 2005. p38-dependent phosphorylation of the mRNA decay-promoting factor KSRP controls the stability of select myogenic transcripts. Mol. Cell **20**:891–903.
8. **Burghes AH, Beattie CE.** 2009. Spinal muscular atrophy: why do low levels of survival motor neuron protein make motor neurons sick? Nat. Rev. Neurosci. **10**:597–609.
9. **Burnett BG, et al.** 2009. Regulation of SMN protein stability. Mol. Cell. Biol. **29**:1107–1115.
10. **Carissimi C, et al.** 2005. Unrip is a component of SMN complexes active in snRNP assembly. FEBS Lett. **579**:2348–2354.
11. **Carissimi C, et al.** 2006. Gemin8 is a novel component of the survival motor neuron complex and functions in small nuclear ribonucleoprotein assembly. J. Biol. Chem. **281**:8126–8134.
12. **Cartegni L, Hastings ML, Calarco JA, de Stanchina E, Krainer AR.** 2006. Determinants of exon 7 splicing in the spinal muscular atrophy genes, SMN1 and SMN2. Am. J. Hum. Genet. **78**:63–77.
13. **Cartegni L, Krainer AR.** 2002. Disruption of an SF2/ASF-dependent exonic splicing enhancer in SMN2 causes spinal muscular atrophy in the absence of SMN1. Nat. Genet. **30**:377–384.
14. **Chari A, et al.** 2008. An assembly chaperone collaborates with the SMN complex to generate spliceosomal snRNPs. Cell **135**:497–509.
15. **Chari A, Paknia E, Fischer U.** 2009. The role of RNP biogenesis in spinal muscular atrophy. Curr. Opin. Cell Biol. **21**:387–393.
16. **Charroux B, et al.** 1999. Gemin3: a novel DEAD box protein that interacts with SMN, the spinal muscular atrophy gene product, and is a component of gems. J. Cell Biol. **147**:1181–1194.
17. **Charroux B, et al.** 2000. Gemin4. A novel component of the SMN complex that is found in both gems and nucleoli. J. Cell Biol. **148**:1177–1186.
18. **Cho S, Dreyfuss G.** 2010. A degron created by SMN2 exon 7 skipping is a principal contributor to spinal muscular atrophy severity. Genes Dev. **24**:438–442.
19. **Coovert DD, et al.** 1997. The survival motor neuron protein in spinal muscular atrophy. Hum. Mol. Genet. **6**:1205–1214.
20. **Corti S, et al.** 2008. Neural stem cell transplantation can ameliorate the phenotype of a mouse model of spinal muscular atrophy. J. Clin. Invest. **118**:3316–3330.
21. **Fischer U, Liu Q, Dreyfuss G.** 1997. The SMN-SIP1 complex has an essential role in spliceosomal snRNP biogenesis. Cell **90**:1023–1029.
22. **Gabanella F, et al.** 2007. Ribonucleoprotein assembly defects correlate with spinal muscular atrophy severity and preferentially affect a subset of spliceosomal snRNPs. PLoS One **2**:e921.
23. **Gavrilov DK, Shi X, Das K, Gilliam TC, Wang CH.** 1998. Differential SMN2 expression associated with SMA severity. Nat. Genet. **20**:230–231.
24. **Gherzi R, et al.** 2004. A KH domain RNA binding protein, KSRP, promotes ARE-directed mRNA turnover by recruiting the degradation machinery. Mol. Cell **14**:571–583.
25. **Gubitz AK, et al.** 2002. Gemin5, a novel WD repeat protein component of the SMN complex that binds Sm proteins. J. Biol. Chem. **277**:5631–5636.
26. **Helmken C, et al.** 2003. Evidence for a modifying pathway in SMA discordant families: reduced SMN level decreases the amount of its interacting partners and Htra2-beta1. Hum. Genet. **114**:11–21.
27. **Hubers L, et al.** 2011. HuD interacts with survival motor neuron protein and can rescue spinal muscular atrophy-like neuronal defects. Hum. Mol. Genet. **20**:553–579.
28. **Jablonka S, et al.** 2002. Gene targeting of Gemin2 in mice reveals a correlation between defects in the biogenesis of U snRNPs and motoneuron cell death. Proc. Natl. Acad. Sci. U. S. A. **99**:10126–10131.
29. **Jodelka FM, Ebert AD, Duelli DM, Hastings ML.** 2010. A feedback loop regulates splicing of the spinal muscular atrophy-modifying gene, SMN2. Hum. Mol. Genet. **19**:4906–4917.
30. **Kashima T, Manley JL.** 2003. A negative element in SMN2 exon 7 inhibits splicing in spinal muscular atrophy. Nat. Genet. **34**:460–463.
31. **Kataoka N, Dreyfuss G.** 2008. Preparation of efficient splicing extracts from whole cells, nuclei, and cytoplasmic fractions. Methods Mol. Biol. **488**:357–365.
32. **Le TT, et al.** 2005. SMNDelta7, the major product of the centromeric survival motor neuron (SMN2) gene, extends survival in mice with spinal muscular atrophy and associates with full-length SMN. Hum. Mol. Genet. **14**:845–857.
33. **Lefebvre S, et al.** 1995. Identification and characterization of a spinal muscular atrophy-determining gene. Cell **80**:155–165.
34. **Lefebvre S, et al.** 1997. Correlation between severity and SMN protein level in spinal muscular atrophy. Nat. Genet. **16**:265–269.
35. **Liu Q, Fischer U, Wang F, Dreyfuss G.** 1997. The spinal muscular atrophy disease gene product, SMN, and its associated protein SIP1 are in a complex with spliceosomal snRNP proteins. Cell **90**:1013–1021.
36. **Lorson CL, Androphy EJ.** 2000. An exonic enhancer is required for inclusion of an essential exon in the SMA-determining gene SMN. Hum. Mol. Genet. **9**:259–265.
37. **Lorson CL, Hahnen E, Androphy EJ, Wirth B.** 1999. A single nucleotide in the SMN gene regulates splicing and is responsible for spinal muscular atrophy. Proc. Natl. Acad. Sci. U. S. A. **96**:6307–6311.
38. **Lunn MR, Wang CH.** 2008. Spinal muscular atrophy. Lancet **371**:2120–2133.
39. **Martins de Araujo M, Bonnal S, Hastings ML, Krainer AR, Valcarcel J.** 2009. Differential 3′ splice site recognition of SMN1 and SMN2 transcripts by U2AF and U2 snRNP. RNA **15**:515–523.
40. **Matera AG, Terns RM, Terns MP.** 2007. Non-coding RNAs: lessons from the small nuclear and small nucleolar RNAs. Nat. Rev. Mol. Cell Biol. **8**:209–220.
41. **McAndrew PE, et al.** 1997. Identification of proximal spinal muscular atrophy carriers and patients by analysis of SMNT and SMNC gene copy number. Am. J. Hum. Genet. **60**:1411–1422.
42. **McGovern VL, Gavrilina TO, Beattie CE, Burghes AH.** 2008. Embryonic motor axon development in the severe SMA mouse. Hum. Mol. Genet. **17**:2900–2909.
43. **Meister G, Buhler D, Pillai R, Lottspeich F, Fischer U.** 2001. A multiprotein complex mediates the ATP-dependent assembly of spliceosomal U snRNPs. Nat. Cell Biol. **3**:945–949.
44. **Monani UR.** 2005. Spinal muscular atrophy: a deficiency in a ubiquitous protein; a motor neuron-specific disease. Neuron **48**:885–896.
45. **Monani UR, et al.** 1999. A single nucleotide difference that alters splicing patterns distinguishes the SMA gene SMN1 from the copy gene SMN2. Hum. Mol. Genet. **8**:1177–1183.
46. **Monani UR, et al.** 2000. The human centromeric survival motor neuron gene (SMN2) rescues embryonic lethality in Smn(−/−) mice and results in a mouse with spinal muscular atrophy. Hum. Mol. Genet. **9**:333–339.
47. **Neuenkirchen N, Chari A, Fischer U.** 2008. Deciphering the assembly pathway of Sm-class U snRNPs. FEBS Lett. **582**:1997–2003.
48. **Olaso R, et al.** 2006. Activation of RNA metabolism-related genes in mouse but not human tissues deficient in SMN. Physiol. Genomics **24**:97–104.
49. **Passini MA, Cheng SH.** 2011. Prospects for the gene therapy of spinal muscular atrophy. Trends Mol. Med. **17**:259–265.

50. **Pearn J.** 1978. Incidence, prevalence, and gene frequency studies of chronic childhood spinal muscular atrophy. J. Med. Genet. **15**:409–413.
51. **Pedrotti S, et al.** 2010. The splicing regulator Sam68 binds to a novel exonic splicing silencer and functions in SMN2 alternative splicing in spinal muscular atrophy. EMBO J. **29**:1235–1247.
52. **Pellizzoni L.** 2007. Chaperoning ribonucleoprotein biogenesis in health and disease. EMBO Rep. **8**:340–345.
53. **Pellizzoni L, Baccon J, Rappsilber J, Mann M, Dreyfuss G.** 2002. Purification of native survival of motor neurons complexes and identification of Gemin6 as a novel component. J. Biol. Chem. **277**:7540–7545.
54. **Pellizzoni L, Yong J, Dreyfuss G.** 2002. Essential role for the SMN complex in the specificity of snRNP assembly. Science **298**:1775–1779.
55. **Prior TW, et al.** 2009. A positive modifier of spinal muscular atrophy in the SMN2 gene. Am. J. Hum. Genet. **85**:408–413.
56. **Russman BS.** 2007. Spinal muscular atrophy: clinical classification and disease heterogeneity. J. Child Neurol. **22**:946–951.
57. **Singh NN, Androphy EJ, Singh RN.** 2004. In vivo selection reveals combinatorial controls that define a critical exon in the spinal muscular atrophy genes. RNA **10**:1291–1305.
58. **Singh NN, Singh RN, Androphy EJ.** 2007. Modulating role of RNA structure in alternative splicing of a critical exon in the spinal muscular atrophy genes. Nucleic Acids Res. **35**:371–389.
59. **Tadesse H, Deschenes-Furry J, Boisvenue S, Cote J.** 2008. KH-type splicing regulatory protein interacts with survival motor neuron protein and is misregulated in spinal muscular atrophy. Hum. Mol. Genet. **17**: 506–524.
60. **Vezain M, et al.** 2010. A rare SMN2 variant in a previously unrecognized composite splicing regulatory element induces exon 7 inclusion and reduces the clinical severity of spinal muscular atrophy. Hum. Mutat. **31**: E1110–1125.
61. **Will CL, Luhrmann R.** 2001. Spliceosomal UsnRNP biogenesis, structure and function. Curr. Opin. Cell Biol. **13**:290–301.
62. **Winkler C, et al.** 2005. Reduced U snRNP assembly causes motor axon degeneration in an animal model for spinal muscular atrophy. Genes Dev. **19**:2320–2330.
63. **Workman E, et al.** 2009. A SMN missense mutation complements SMN2 restoring snRNPs and rescuing SMA mice. Hum. Mol. Genet. **18**: 2215–2229.
64. **Zhang Z, et al.** 2008. SMN deficiency causes tissue-specific perturbations in the repertoire of snRNAs and widespread defects in splicing. Cell **133**: 585–600.